

CD8 α^+ β^- and CD8 α^+ β^+ plasmacytoid dendritic cells induce Foxp3 $^+$ regulatory T cells and prevent the induction of airway hyper-reactivity

V Lombardi¹, AO Speak¹, J Kerzerho¹, N Szely¹ and O Akbari¹

Dendritic cells (DCs) control the balance between protection against pathogens and tolerance to innocuous or self-antigens. Here, we demonstrate for the first time that mouse plasmacytoid DCs (pDCs) can be segregated into three distinct populations, exhibiting phenotypic and functional differences, according to their surface expression of CD8 α or CD8 β as CD8 α^- β^- , CD8 α^+ β^- , or CD8 α^+ β^+ . In a mouse model of lung inflammation, adoptive transfer of CD8 α^+ β^- or CD8 α^+ β^+ pDCs prevents the development of airway hyper-reactivity. The tolerogenic features of these subsets are associated with increased production of retinoic acid, which leads to the enhanced induction of Foxp3 $^+$ regulatory T cells compared with CD8 α^- β^- pDCs. Our data thus identify subsets of pDCs with potent tolerogenic functions that may contribute to the maintenance of tolerance in mucosal sites such as the lungs.

INTRODUCTION

Dendritic cells (DCs) constitute a family of cells with the unique ability to distinguish pathogens from innocuous microorganisms as well as self from non-self antigens.^{1,2} These cells can further initiate a robust immune response to infectious agents or in contrast, maintain immune tolerance to innocuous or self-antigens. To accomplish these tasks, DCs are equipped with pattern recognition receptors that recognize motifs highly conserved in pathogens throughout the evolution.³ Engagement of these receptors triggers the upregulation of co-stimulatory molecules and the production of immune mediators such as cytokines. Along with the capacity of DCs to present antigen, these signals direct the differentiation of naïve CD4 $^+$ T cells into the appropriate subset of T helper (Th) cells.^{2,4,5} Therefore, DCs are key regulators of the immune system considering their ability to control the balance between immunity and tolerance.^{2,4} How DCs achieve these apparently opposite functions remains elusive and many studies suggest that immunogenic and tolerogenic functions are assigned to different subpopulations of DCs.^{2,4-6}

DCs can be divided into two populations that express different cell surface markers, morphology, migratory routes, and exhibit different functional properties.⁷ Conventional DCs (cDCs) can be defined by their CD11c $^{\text{hi}}$ major histocompatibility complex class II $^{\text{hi}}$ phenotype, whereas plasmacytoid

DCs (pDCs) are identified as CD11c $^{\text{low}}$ major histocompatibility complex class II $^{\text{dim}}$ CD45R/B220 $^+$ BST2/mPDCA-1 $^+$.⁸ Increasing evidence suggests that pDCs are vital mediators of anti-viral immunity in part due to their expression of receptors specialized for the recognition of pathogen-derived nucleic acids (toll-like receptor (TLR) 7 and 9) and rapid release of type I interferons (IFNs) after activation by TLR engagement.⁹ However, it is now becoming evident that pDCs are also key mediators of tolerance in mucosal sites. For example, depletion of pDCs prevents the establishment of respiratory tolerance¹⁰ and adoptive transfer of pDCs can reduce established lung inflammation in animal models.¹¹ In an oral tolerance model, pDCs have been shown to be essential for the presentation of dietary antigens¹² and their role in the induction of tolerance to transplanted grafts has been suggested.^{13,14} However, all these studies have used total pDC populations and the identification or functional description of pDC subsets has not been elucidated as it has been previously described for many subsets of cDCs in the induction of tolerance. For instance, the gut-associated lymphoid tissue contains a subset of DCs, defined by expression of the mucosal integrin CD103, that have immunoregulatory properties.¹⁵ These cells are able to promote the differentiation of Foxp3 $^+$ regulatory T cells (T $_{\text{reg}}$) cells from naïve CD4 $^+$ T cells. In the lungs, under normal conditions, respiratory exposure to

¹Department of Molecular Microbiology and Immunology, Keck School of Medicine, University of Southern California, Los Angeles, California, USA. Correspondence: O Akbari (akbari@usc.edu)

Received 30 August 2011; accepted 8 February 2012; published online 4 April 2012. doi:10.1038/mi.2012.20

antigen elicits the generation of tolerogenic cDCs and Foxp3⁺ T_{reg} cells resulting in immune tolerance.^{16–18} In addition to the tolerogenic function of pDCs and cDCs, mucosal tissues also contain a specialized microenvironment that is required for the induction and maintenance of tolerance. In the gut, CD103⁺ DCs release retinoic acid, which increases the transforming growth factor- β (TGF- β)-mediated conversion of naïve CD4⁺ T cells into Foxp3⁺ T_{reg} cells.^{15,19} Retinoic acid is generated from vitamin A in a two-step process catalyzed by alcohol dehydrogenase and then retinal dehydrogenase (RALDH), and is known to be a potent immunoregulatory compound.²⁰ Previous studies examining the expression and activity of RALDH enzymes in DCs demonstrated that cDCs isolated from mucosal sites possess greatly enhanced RALDH activity compared with spleen cDCs.²¹ A deregulation of mucosal tolerance can lead to the development of immune disorders such as allergic diseases, inflammatory bowel disease, and asthma.^{5,22}

Herein, we demonstrate for the first time that pDCs can express CD8 α alone or in combination with CD8 β and can be segregated into three subpopulations, CD8 α ⁻ β ⁻, CD8 α ⁺ β ⁻, and CD8 α ⁺ β ⁺. These subsets of pDCs demonstrate differential cytokine secretion and functional properties both *in vitro* and *in vivo*. Adoptive transfer of CD8 α ⁻ β ⁻ pDCs triggered sensitization when transferred into naïve mice, whereas CD8 α ⁺ β ⁻ and CD8 α ⁺ β ⁺ pDCs exhibited poor capacity for sensitization. In contrast with using a model of airway inflammation, adoptive transfer of CD8 α ⁺ β ⁻ and CD8 α ⁺ β ⁺ pDCs prevents the development of airway hyper-reactivity (AHR). Therefore, CD8 α ⁺ β ⁻ or CD8 α ⁺ β ⁺ pDCs can induce tolerance *in vivo*. One potential mechanism for this observation is the induction of T_{reg} cells. We have discovered that CD8 α ⁺ β ⁻ or CD8 α ⁺ β ⁺ pDCs strongly support the differentiation of Foxp3⁺ CD4⁺ T_{reg} cells both *in vivo* and *in vitro*. The ability of tolerogenic pDC subsets to induce T_{reg} cells is associated with the increased expression of *Aldha1a1*, *Aldha1a2*, and *Aldha1a3* genes encoding RALDH1, RALDH2, and RALDH3 enzymes, respectively. Inhibition of RALDH activity prevents the induction of Foxp3⁺ T_{reg} cells by CD8 α ⁺ β ⁻ or CD8 α ⁺ β ⁺ pDCs. Therefore, our data show that CD8 α and CD8 β can define subpopulations of pDCs, which possess either tolerogenic (CD8 α ⁺ β ⁻ or CD8 α ⁺ β ⁺) or pro-inflammatory (CD8 α ⁻ β ⁻) properties.

RESULTS

A subset of pDCs express CD8 α or CD8 $\alpha\beta$

In a selection of organs (spleen, peripheral lymph nodes, and lungs), we analyzed by flow cytometry the expression of an assortment of myeloid and lymphoid markers on the plasmacytoid population of DCs, to identify subsets of pDCs. We observed expression of CD8 α and CD8 β on pDCs, which can define three subsets: CD8 α ⁻ β ⁻, CD8 α ⁺ β ⁻, and CD8 α ⁺ β ⁺ (Figure 1a). To confirm our findings by flow cytometry, we performed several staining controls (Supplementary Figure S1a online) and used two different clones specific for CD8 β (H35-17.2 and 53-5.8) with similar results obtained with both clones (data not shown). These findings were validated by fluo-

rescent confocal microscopy analysis of pDCs purified from peripheral lymph nodes and stained with mPDCA1, anti-IA/IE, or anti-CD11c in addition to CD8 α and CD8 β (Figure 1b). We showed that a subset of pDCs express CD8 α alone or associated with CD8 β (Figure 1b). Depending on the tissue analyzed, CD8 α ⁺ β ⁻ pDCs represent 10–22% of pDCs and CD8 α ⁺ β ⁺ pDCs 4–23% of the whole population of pDCs (Figure 1c). The three subsets of pDCs described herein exhibit all the specific markers of terminally differentiated pDCs (positive for mPDCA1, Siglec-H, Ly6C, B220, and Ly49Q) and display an immature phenotype with a low expression of co-stimulatory molecules CD40, CD80, CD86, PD-L1, PD-L2, ICOS-L, and OX40-L (Figure 1d). To test whether *in vivo* expansion of DCs affects the expression of CD8 α or CD8 β at the surface of pDCs, Renca tumor cells expressing Fms-like tyrosine kinase 3-ligand (Flt3-L) were subcutaneously injected into BALB/c mice. Flt3-L acts on hematopoietic stem cells and controls their differentiation into DCs; this treatment expands the population of DCs by 15- to 20-fold after 14 days without activating the cells.²³ We observed that Flt3-L treatment does not significantly affect the level of expression of CD8 α and CD8 β on pDCs (Supplementary Figure 1b online). The expression of CD8 α and CD8 β was assessed simultaneously on pDCs (CD11c^{dim} mPDCA1⁺ cells) and on cDCs (CD11c^{high} mPDCA1⁻ cells). At the surface of cDCs, only CD8 α expression was detected (Supplementary Figure S1b online). To prevent any irrelevant signal coming from CD8-expressing T cells, DCs were gated on CD11c⁺ cells, while T cells were excluded in the gating strategy by CD3 staining (Supplementary Figure S1b online). To confirm our results, we sorted each subset by flow cytometry (cell sorting purity is presented in Supplementary Figure S2a online) and assessed the gene expression of *Cd8a* and *Cd8b* genes by real-time PCR. In agreement with the surface phenotype, *Cd8a* gene expression was detected in CD8 α ⁺ β ⁻ pDCs, whereas both *Cd8a* and *Cd8b* genes were strongly expressed in the CD8 α ⁺ β ⁺ subset (Figure 2a). As expected, *Cd8b* gene expression was never detected in cDCs. To examine if the surface expression of CD8 α or CD8 β is due to the possible uptake of CD8 antigens from CD8⁺ T cells,²⁴ we analyzed the expression of CD8 α and CD8 β in pDCs from β 2 microglobulin knockout (B2m^{-/-}) mice. These mice lack cell surface major histocompatibility complex class I expression and thus CD8⁺ T cells.²⁵ The pDCs from B2m^{-/-} animals exhibited the same profile of CD8 α and CD8 β expression as wild-type controls demonstrating the *bona fide* expression of these proteins by pDCs (Figure 2b). Furthermore, this was confirmed by quantitative real-time PCR after isolation of each subpopulation by cell sorting (Figure 2c). Collectively, these data confirm that pDCs express CD8 α or CD8 $\alpha\beta$ and can be divided into three subsets accordingly.

CD8 α ⁻ β ⁻, CD8 α ⁺ β ⁻, and CD8 α ⁺ β ⁺ pDCs present distinct cytokine production, antigen uptake, and priming properties

The main function of DCs is to prime naïve T cells by presenting antigen and providing additional signals through co-stimulatory molecules and production of cytokines. To address whether the

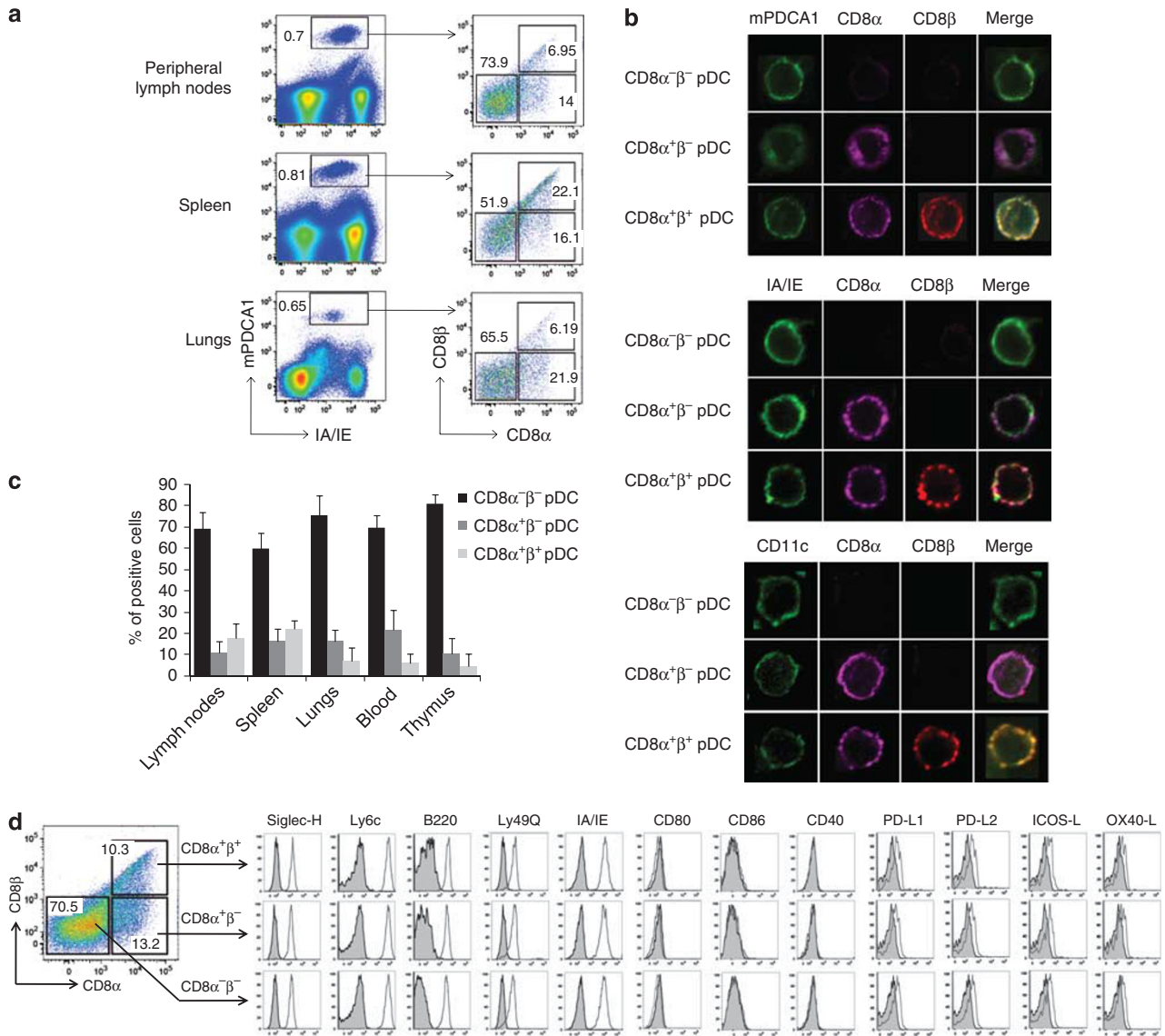


Figure 1 Plasmacytoid dendritic cells (pDCs) express either CD8α or CD8αβ. **(a)** Cells prepared from peripheral lymph nodes, spleen, or lungs of naïve mice were stained with anti-IA/IE, mPDCA1, anti-CD8α, and anti-CD8β antibodies. CD8α and CD8β surface expression was analyzed by flow cytometry on pDCs gated according to mPDCA1 and IA/IE staining. Gates were set based on isotype controls; numbers in outlined areas indicate the percentage of positive cells in the designated region. Representative dot plots from five experiments are shown. **(b)** pDCs magnetically purified from peripheral lymph nodes of naïve mice were stained with mPDCA1, anti-IA/IE, or anti-CD11c along with CD8α and CD8β antibodies and analyzed by fluorescence confocal microscopy. Original magnification ×1,000. **(c)** Percentage of CD8α⁻β⁻, CD8α⁺β⁻, and CD8α⁺β⁺ pDCs in peripheral lymph nodes, spleen, lungs, blood, and thymus. Data are from two independent experiments (mean±s.e.m.). **(d)** Surface expression of Siglec-H, Ly6c, B220, Ly49Q, IA/IE, CD80, CD86, CD40, PD-L1, PD-L2, ICOS-L, and OX40-L was assessed by flow cytometry on CD8α⁻β⁻ pDCs, CD8α⁺β⁻ pDCs, and CD8α⁺β⁺ pDCs from peripheral lymph nodes. Shaded histograms represent isotype control antibodies; solid black lines represent specific stainings. Data are representative of three independent experiments.

subsets of pDCs described herein differ in these functions, we stimulated them with TLR ligands and assessed the expression of co-stimulatory molecules along with the cytokine production. We stimulated CD8α⁻β⁻, CD8α⁺β⁻, and CD8α⁺β⁺ pDCs with R848 (synthetic TLR7 ligand) and CpG oligonucleotides (TLR9 ligand) and assessed the production of IFN-α, tumor necrosis factor-α, interleukin (IL)-6, and IL-10. pDCs are known to produce large amount of type I IFN in response to a viral infection, and also are reported to produce significant levels

of IL-6 and IL-10.^{8,26–28} We observed that, after activation via either TLR7 or TLR9, the expression of CD8α or CD8β is not altered and we did not detect any difference in the upregulation of co-stimulatory molecules between the three subsets (data not shown). Interestingly, it appeared that CD8α⁻β⁻ produce more IFN-α, tumor necrosis factor-α, IL-6, and IL-10 than CD8α⁺β⁻ and CD8α⁺β⁺ pDCs upon stimulation (**Figure 3a**), despite a similar expression of TLR7 and 9 (data not shown). We next tested the antigen uptake capacity of the pDCs using a

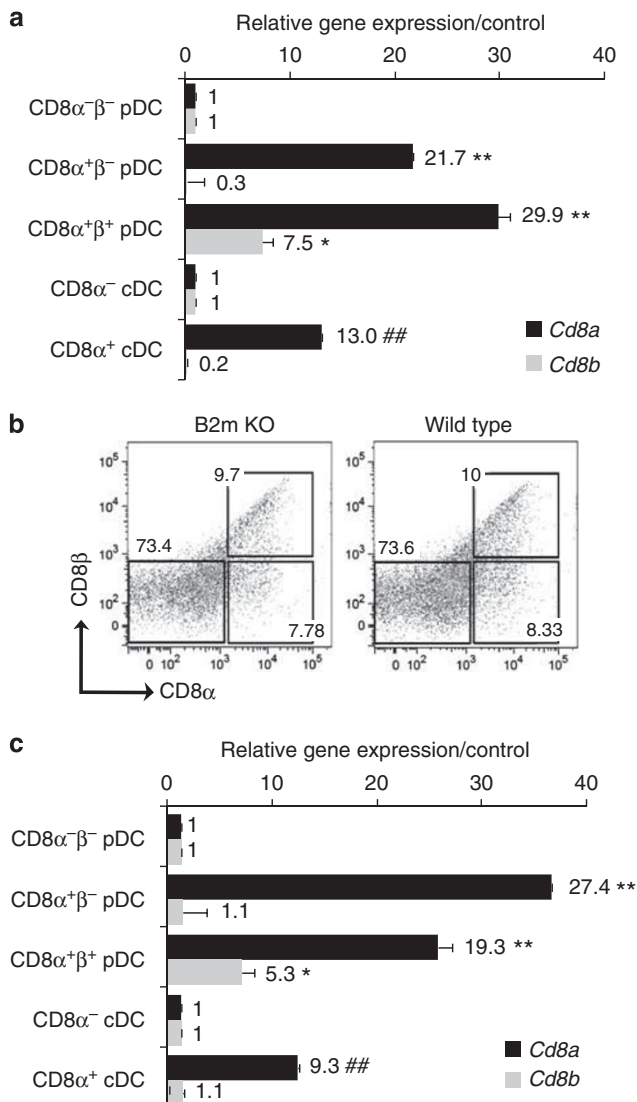


Figure 2 CD8 α and CD8 β are co-expressed on a subset of plasmacytoid dendritic cells (pDCs) but not on conventional dendritic cells (cDCs). (a) CD8 α ⁻β⁻, CD8 α ⁺β⁻, and CD8 α ⁺β⁺ pDCs from peripheral lymph nodes or splenic CD8 α ⁻ and CD8 α ⁺ cDCs were sorted by flow cytometry from Fms-like tyrosine kinase 3-ligand (Flt3-L)-treated mice before isolation of total RNA. Relative gene expression of *Cd8a* and *Cd8b* genes was assessed by quantitative real-time PCR. CD8 α ⁻β⁻ pDCs were used as a calibrator to evaluate *Cd8a* and *Cd8b* gene expression in CD8 α ⁺β⁻ and CD8 α ⁺β⁺ pDCs, whereas CD8 α ⁻ cDCs served as a reference to measure *Cd8a* and *Cd8b* gene expression in CD8 α ⁺ cDCs. Data are the average \pm s.e.m. of six independent experiments. (b) CD8 α and CD8 β surface expression was assessed by flow cytometry in B2m^{-/-} mice lacking CD8 β T cells. pDCs from pooled peripheral lymph nodes of Flt3-L-treated wild-type or B2m^{-/-} mice were stained with CD8 α and CD8 β specific antibodies and analyzed by flow cytometry. Gates were defined using isotype controls and numbers in outlined areas represent the percentage of positive cells for each population. Data are representative of two experiments. (c) Expression of *Cd8a* and *Cd8b* genes was tested by real-time PCR in CD8 α ⁻β⁻, CD8 α ⁺β⁻, and CD8 α ⁺β⁺ pDCs or splenic CD8 α ⁻ and CD8 α ⁺ cDCs isolated by cell sorting from Flt3-L-treated B2m^{-/-} mice. Data are the mean \pm s.e.m. of three different experiments. *P*-values were calculated with Student's *t*-test. **P*-value < 0.05, ***P*-value < 0.02 (compared to CD8 α ⁻β⁻ pDCs). ##*P*-value < 0.02 (compared to CD8 α ⁻ cDCs). B2m KO, β 2 microglobulin knockout.

fluorescent antigen (ovalbumin-antigen-presenting cell (OVA-APC)) in a flow cytometry-based assay. CD8 α ⁺β⁺ pDCs have an enhanced capacity to endocytose antigen compared with CD8 α ⁺β⁻ and CD8 α ⁻β⁻ pDCs, which demonstrated an intermediate and low uptake capacity, respectively (Figure 3b). We then explored whether the three subtypes of pDCs described in this study have a different ability to prime CD4⁺ T cells. We performed an *in vitro* co-culture between these subsets of pDCs and CD4⁺ T cells isolated from DO11.10 mice with an OVA-specific transgenic T-cell receptor. In response to OVA, we observed a robust proliferation when CD8 α ⁻β⁻ pDCs were used as the APCs (Figure 3c). In contrast, CD8 α ⁺β⁻ pDCs and CD8 α ⁺β⁺ pDCs poorly supported the proliferation of CD4⁺ T cells in response to antigen stimulation *in vitro* (Figure 3c). As expected, the production of IL-2 was correlated with the trends observed during the proliferation assay (Figure 3c). Therefore, these pDC subsets segregated according to their expression of CD8 α or CD8 β exhibit striking differences in their capacity to trigger the proliferation of naïve CD4⁺ T cells, to produce cytokines or to uptake antigens.

Transfer of CD8 α ⁻β⁻ pDCs triggers the development of airway inflammation

As demonstrated above, these pDC subsets exhibit differential ability to process and present antigens and to activate CD4⁺ T cells *in vitro*. We therefore wanted to test the functional capacity of these pDC subsets to confer antigen sensitization *in vivo* using a model of AHR. Thus, we sorted pDC subsets from mice treated with Flt3-L, loaded them with OVA, and adoptively transferred these cells or OVA-loaded bone marrow-derived DCs as a positive control, into naïve mice. Mice were challenged intranasally with antigen 1 week later (Figure 4a). Lung inflammation was assessed by evaluating AHR by plethysmography and lung histology. In agreement with the *in vitro* ability to activate T cells, adoptive transfer of CD8 α ⁻β⁻ pDCs supported the robust development of AHR as determined by lung resistance (R_L) and dynamic compliance (C_{dyn}) in anesthetized, tracheotomized, and ventilated animals or as enhance pause (Penh) in conscious animals (Figure 4b and c). In contrast, CD8 α ⁺β⁻ and CD8 α ⁺β⁺ pDCs, which demonstrated poor ability to induce T-cell proliferation *in vitro*, did not trigger significant AHR (Figure 4b and c). We then examined lung histology to support the lung function data. Lung sections were stained with hematoxylin and eosin to observe cellular infiltration or periodic acid Schiff to examine mucus production. In accordance with the plethysmography results, a massive cell infiltration as well as significant mucus production was observed in mice transferred with CD8 α ⁻β⁻ pDCs (Figure 4d). In contrast, only minor cellular infiltration and no mucus secretion was observed after transfer of CD8 α ⁺β⁻ pDCs, whereas lungs of mice that received cDCs did not present considerable abnormalities (Figure 4d). These results collectively show that CD8 α ⁻β⁻ pDCs can be considered as an immunogenic population of pDCs in contrast with CD8 α ⁺β⁻ or CD8 α ⁺β⁺ pDCs.

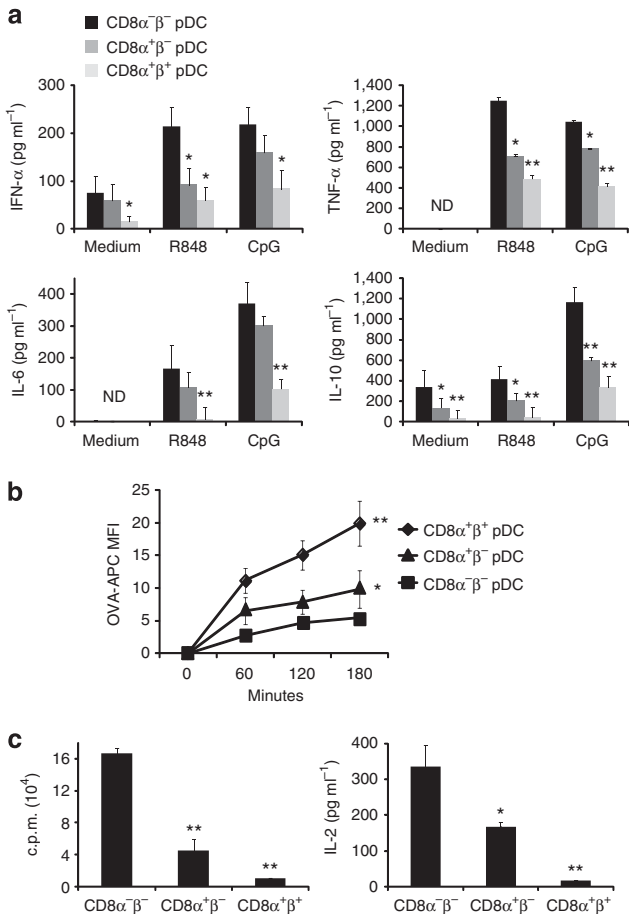


Figure 3 CD8 $\alpha^+\beta^-$ and CD8 $\alpha^+\beta^+$ plasmacytoid dendritic cells (pDCs) produce low amount of cytokines and weakly prime naive CD4 $^+$ T cells. **(a)** pDC subsets were sorted by flow cytometry from peripheral lymph nodes of mice treated with Fms-like tyrosine kinase 3-ligand (Flt3-L) according to their expression of CD8 α or CD8 $\alpha\beta$. CD8 $\alpha^-\beta^-$, CD8 $\alpha^+\beta^-$, and CD8 $\alpha^+\beta^+$ pDCs were subsequently stimulated *in vitro* with R848 (1 $\mu\text{g ml}^{-1}$) or CpG (1 μM) for 24 h. Culture supernatants were tested for interferon- α (IFN- α), interleukin (IL)-6, tumor necrosis factor- α (TNF- α), and IL-10 by enzyme-linked immunosorbent assay (ELISA). Results are average \pm s.e.m. of two independent experiments. **(b)** pDC subsets were cultured for 60, 120, or 180 min in the presence of ovalbumin-antigen-presenting cell (OVA-APC) (10 $\mu\text{g ml}^{-1}$) at 37 $^\circ\text{C}$ or 4 $^\circ\text{C}$. Cells were then washed and stained with CD8 α and CD8 β antibodies. APC fluorescence was analyzed by flow cytometry in CD8 $\alpha^-\beta^-$, CD8 $\alpha^+\beta^-$, or CD8 $\alpha^+\beta^+$ pDC subpopulations. Data are average of ((mean fluorescence intensity (MFI) at 37 $^\circ\text{C}$) - (MFI at 4 $^\circ\text{C}$)) \pm s.e.m. of three separate experiments. **(c)** Naive CD4 $^+$ T cells from DO11.10 mice were co-cultured with CD8 $\alpha^-\beta^-$, CD8 $\alpha^+\beta^-$, or CD8 $\alpha^+\beta^+$ pDCs. Cells were cultured for 3 days at a 1:10 ratio (pDCs:CD4 $^+$ T cells) with 10 $\mu\text{g ml}^{-1}$ of OVA before being pulsed for 18 h with ^3H thymidine. Incorporation of radioactivity was determined by liquid scintillation counting. Alternatively, supernatants were collected and tested for IL-2 by ELISA. Results are the mean of triplicates \pm s.e.m. of one representative experiment out of two. *P*-values were determined using the Student's *t*-test. **P*-value < 0.05; ***P*-value < 0.02 (compared to CD8 $\alpha^-\beta^-$ pDCs). c.p.m., counts per minute.

CD8 $\alpha^+\beta^-$ or CD8 $\alpha^+\beta^+$ pDCs prevents AHR and inflammation
As CD8 $\alpha^+\beta^-$ and CD8 $\alpha^+\beta^+$ pDC subsets demonstrated poor immunogenic capacity *in vitro* and *in vivo*, we hypothesized

that these subsets may exhibit tolerogenic properties *in vivo*. To examine this possibility, the three subsets of pDCs were initially loaded with OVA and adoptively transferred to naive mice that were subsequently sensitized and challenged (Figure 5a). We observed that respiratory function of mice transferred with CD8 $\alpha^+\beta^-$ pDCs and more especially CD8 $\alpha^+\beta^+$ pDCs were significantly improved (Figure 5b). In contrast, animals that received CD8 $\alpha^-\beta^-$ pDCs demonstrated a robust induction of AHR that was indistinguishable to the positive control group (mice that received saline solution) (Figure 5b). Accordingly, analysis of lung histology showed that only mice treated with CD8 $\alpha^-\beta^-$ pDCs exhibited a high cellular infiltration and mucus secretion characteristic of airway inflammation (Figure 5c). We also demonstrated that in mice treated with either CD8 $\alpha^+\beta^-$ or CD8 $\alpha^+\beta^+$ pDCs, the production of Th2 cytokines IL-4 and IL-13 is reduced significantly compared with sensitized mice (Figure 5d). Similarly, levels of OVA-specific immunoglobulin G and immunoglobulin E were diminished in mice, which received either CD8 $\alpha^+\beta^-$ or CD8 $\alpha^+\beta^+$ pDCs (Figure 5e). Therefore, CD8 $\alpha^+\beta^+$ and CD8 $\alpha^+\beta^-$ pDCs promote the development of immune tolerance as shown by their ability to prevent lung inflammation and can therefore be classified as *bona fide* tolerogenic pDC subsets.

CD8 $\alpha^+\beta^-$ and CD8 $\alpha^+\beta^+$ pDCs promote the differentiation of antigen-specific CD4 $^+$ CD25 $^+$ Foxp3 $^+$ T cells *in vivo*

Tolerance may be achieved by multiple mechanisms, including induction of Foxp3 $^+$ T $_{\text{reg}}$ cells, which suppress the activity of antigen-specific effector T cells.²⁹ We therefore sought to determine the mechanism that allows CD8 $\alpha^+\beta^-$ and CD8 $\alpha^+\beta^+$ pDCs to induce T-cell tolerance *in vivo*. To test the ability of these pDC subsets to induce the conversion of naive CD4 $^+$ T cells into Foxp3 $^+$ T $_{\text{reg}}$ cells, we performed an *in vivo* adoptive transfer study. We co-transferred naive CD4 $^+$ CD62L $^+$ Foxp3 $^-$ T cells isolated from OVA-specific DO11.10 mice with the different OVA-loaded pDC subsets into naive mice (purity of naive CD4 $^+$ T cells; Supplementary Figure S2c and d online). After 4 days, we challenged the mice intranasally with OVA to recruit T cells to the lungs and then analyzed Foxp3 expression in the spleen and lungs by flow cytometry. We tracked the conversion of OVA-specific CD4 $^+$ T cells into Foxp3-expressing cells using the clonotypic antibody KJ1.26 specific of the OVA-specific transgenic T-cell receptor³⁰ (Figure 6a). The percentage of CD4 $^+$ KJ1.26 $^+$ CD25 $^+$ Foxp3 $^+$ T cells was significantly increased in mice that received CD8 $\alpha^+\beta^-$ or CD8 $\alpha^+\beta^+$ pDCs (Figure 6b). With the transfer of this last subset, the percentage of CD4 $^+$ CD25 $^+$ Foxp3 $^+$ T cells was increased by twofold in the lungs compared with transfer of CD8 $\alpha^-\beta^-$ pDCs. Therefore, CD8 $\alpha^+\beta^-$ and CD8 $\alpha^+\beta^+$ pDCs possess the capacity to induce antigen-specific CD4 $^+$ CD25 $^+$ Foxp3 $^+$ T $_{\text{reg}}$ cells *in vivo*.

RALDH expression in CD8 $\alpha^+\beta^-$ or CD8 $\alpha^+\beta^+$ pDCs is responsible for induction of T $_{\text{reg}}$

The induction of T $_{\text{reg}}$ cells *in vivo* by tolerogenic DCs has previously been demonstrated to be regulated by TGF- β and

retinoic acid.³¹ To test the role of retinoic acid, we analyzed the gene expression of the aldehyde dehydrogenase enzymes (RALDH) that catalyze one step of the conversion of retinol into retinoic acid. We determined that *Aldha1a1*, *Aldha1a2*, and *Aldha1a3*, three genes encoding RALDH1, RALDH2, and RALDH3 enzymes, respectively, were upregulated in the tolerogenic CD8 α^+ β^- or CD8 α^+ β^+ pDC subsets (**Figure 7a**). As a control, we tested simultaneously the expression of these genes in CD103 $^+$ cDCs from mesenteric lymph nodes that have previously been demonstrated to induce Foxp3 $^+$ T $_{reg}$ cells in a retinoic acid-dependent manner.^{15,19} In accordance with previous reports, CD103 $^+$ cDCs expressed high levels of *Aldha1a1* and *Aldha1a2* compared with CD103 $^-$ cDCs, but did not express *Aldha1a3* in contrast to the pDC subsets described herein (**Figure 7a**). To demonstrate the functional activity of RALDH in pDCs, we used the fluorescent RALDH substrate, Aldefluor, in a flow cytometry assay, as has been demonstrated

previously.^{21,32} In agreement with the hierarchy of T $_{reg}$ induction capacity *in vivo* and *Aldha* genes expression, CD8 α^+ β^+ pDC demonstrated the highest RALDH activity and CD8 α^- β^- the lowest (**Figure 7b**). We next tested the requirements for TGF- β and retinoic acid in the conversion of naïve T cells into T $_{reg}$ cells by pDC subsets *in vitro*. We cultured pDC subsets with naïve OVA-specific CD4 $^+$ T cells in the presence or absence of TGF- β or TGF- β and RALDH inhibitor (LE540).^{31,33} We observed that, in the presence of TGF- β , CD8 α^+ β^+ and CD8 α^+ β^- pDCs are more efficient in converting naïve CD4 $^+$ T cells into Foxp3-expressing T $_{reg}$ cells compared with CD8 α^- β^- pDCs (**Figure 7c**). In addition, the presence of an RALDH inhibitor completely blocked the conversion of naïve CD4 $^+$ T cells by CD8 α^+ β^+ and CD8 α^+ β^- pDCs (**Figure 7c**). Altogether, these results demonstrate that CD8 α^+ β^- pDCs and in particular CD8 α^+ β^+ pDCs strongly support the development of Foxp3 $^+$ CD4 $^+$ T $_{reg}$ cells in a TGF- β - and retinoic acid-dependent manner.

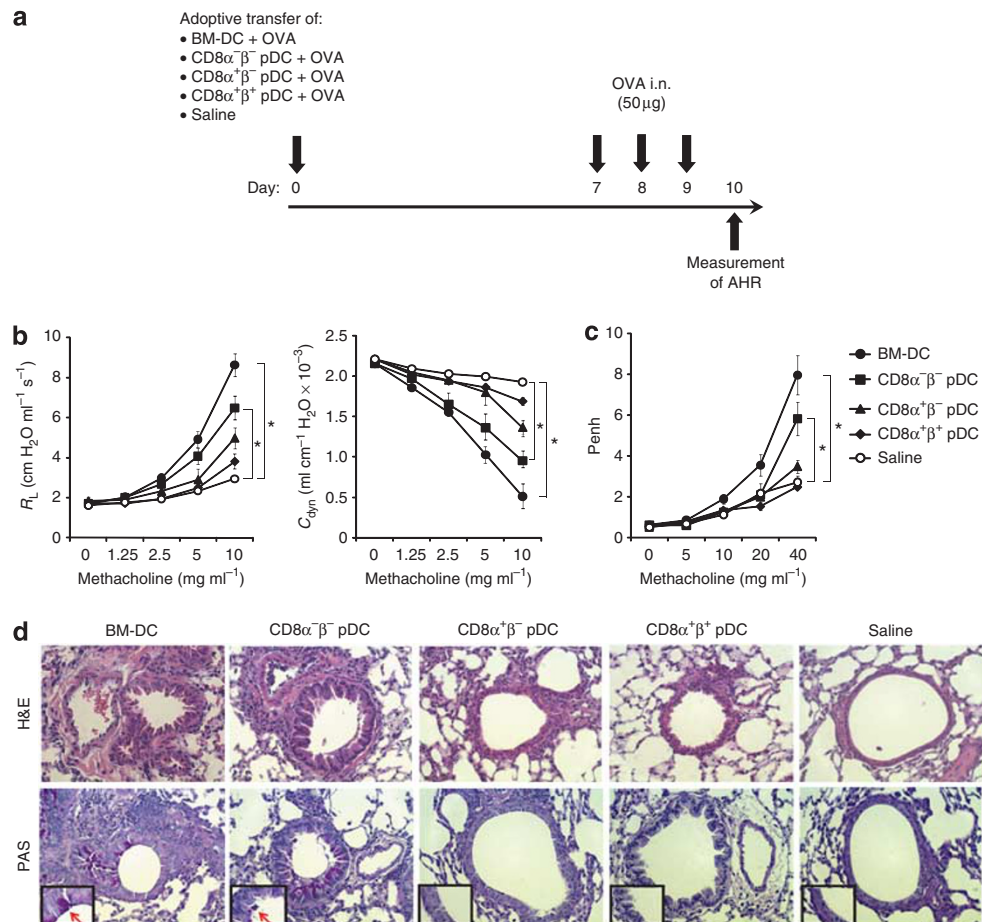
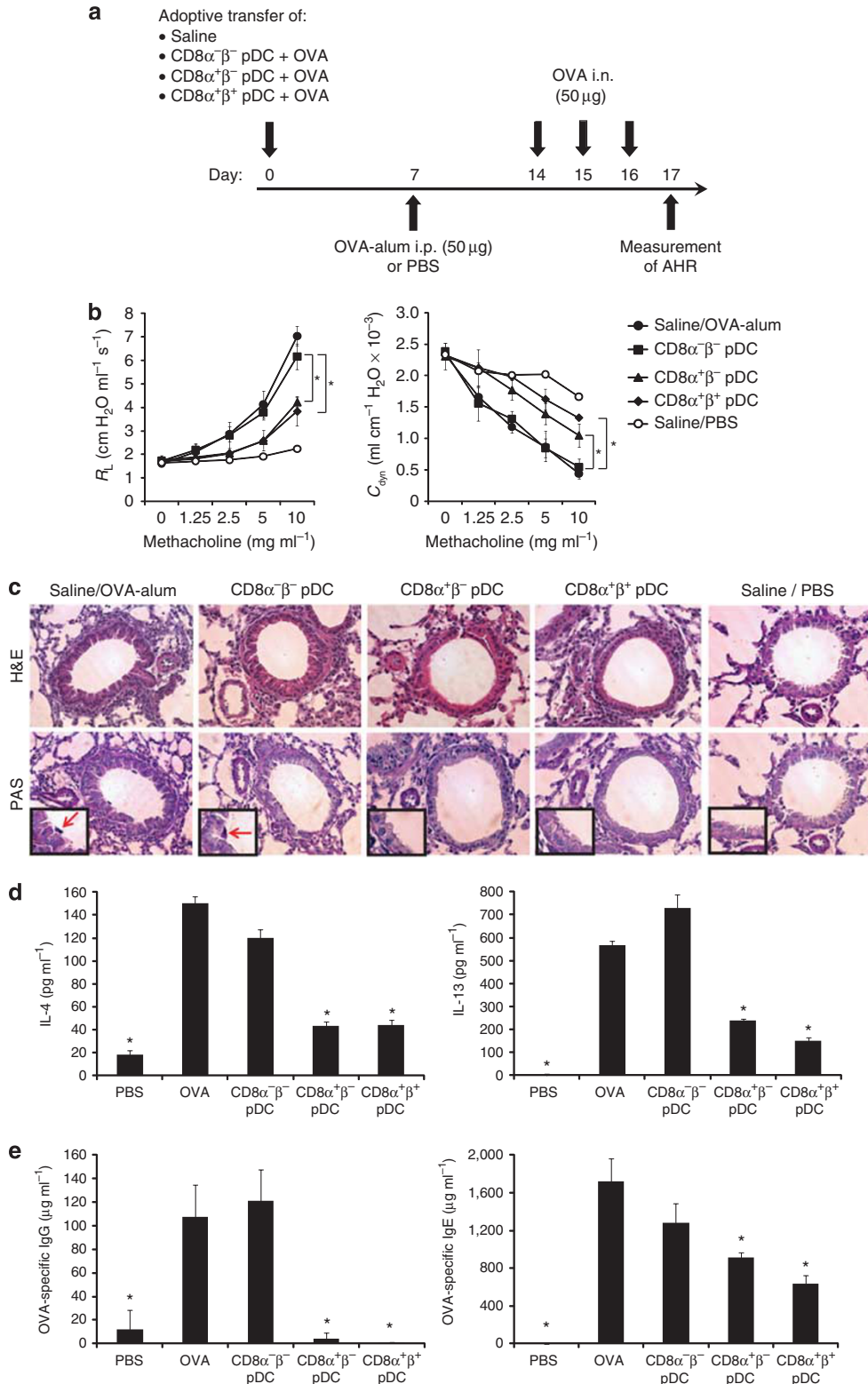


Figure 4 CD8 α^- β^- plasmacytoid dendritic cells (pDCs) promote the development of airway hyper-reactivity (AHR). (**a**) pDC subsets isolated by cell sorting from peripheral lymph nodes of Fms-like tyrosine kinase 3-ligand (Flt3-L)-treated mice or bone marrow-derived DCs (BM-DCs) were loaded with ovalbumin (OVA) (10 μ g ml $^{-1}$) for 4 h and then adoptively transferred into naïve BALB/c mice (2×10^5 cells per mouse). After 7 days, mice were challenged by intranasal (IN) administration of OVA (50 μ g in 50 μ l phosphate-buffered saline (PBS)) on three consecutive days. (**b**) AHR was subsequently assessed by plethysmography to measure lung resistance (R_L), dynamic compliance (C_{dyn}), and (**c**) enhanced pause (Penh). Data are average \pm s.e.m. of groups of five mice of one representative experiment out of two. * $P < 0.05$ as determined by two-tailed Student's *t*-test. (**d**) Representative lung histology of mice from panel **c**. Lung tissue from mice transferred with CD8 α^- β^- pDCs, CD8 α^+ β^- pDCs, CD8 α^+ β^+ pDCs, or BM-DCs were stained with hematoxylin and eosin (H&E, upper panel) and periodic acid Schiff (PAS, lower panel). Arrows show the release of the mucus in the lumen. Original magnification $\times 200$, inset $\times 600$.

DISCUSSION

In this study, we demonstrate for the first time that pDCs can express either CD8 α or co-express CD8 α and CD8 β , thus defining three populations of pDCs: CD8 α ⁻β⁻, CD8 α ⁺β⁻, and CD8 α ⁺β⁺. These subsets express all the markers char-

acteristic of terminally differentiated immature pDCs and possess a similar expression of co-stimulatory molecules. However, these three pDC subsets exhibited striking differences in their functional capacity to uptake antigen, produce cytokines after activation, and prime naïve CD4⁺ T cells. Furthermore, we



have determined *in vivo* that CD8 α ⁻β⁻ pDCs are immunogenic, whereas CD8 α ⁺β⁻ and CD8 α ⁺β⁺ pDCs exhibited tolerogenic properties. This is associated with the ability of CD8 α ⁺β⁻ and

CD8 α ⁺β⁺ pDCs to support very effectively the conversion of naïve CD4⁺ T cells into Foxp3⁺ T_{reg} cells both *in vivo* and *in vitro*. Tolerogenic subsets of pDCs express three isoforms of RALDH enzymes and blocking the activity of these enzymes was shown to be essential for this conversion to occur. Our findings thus suggest that the expression of CD8 α or CD8 α β by pDCs define three subsets of cells exhibiting different functions and that CD8 α ⁺β⁻ and CD8 α ⁺β⁺ pDCs demonstrate *bona fide* tolerogenic properties.

There is strong evidence that pDCs have critical roles in induction of peripheral tolerance. For example, pDCs are essential to maintain tolerance in the lungs^{10,11} and digestive tract.¹² In addition, pDCs have been shown to offer therapeutic benefit in murine models of graft vs. host disease^{13,14} and lung inflammation.¹⁰ Induction of tolerance is important in mucosal tissues in terms of immune responses to antigens encountered in the respiratory and intestinal tracts. These sites are continuously exposed to a wide variety of environmental, nonpathogenic antigens, which induce immune tolerance or hyporesponsiveness rather than active immunity.^{34,35} Thus, under normal circumstances, food allergen in the intestinal tract or inhaled allergens in the airways generally do not induce protective immune responses. However, in individuals with allergic asthma, processing of these proteins result in the induction of antigen-specific Th2-biased inflammatory responses that cause AHR and asthma.⁵ The specific events that alter antigen processing and presentation in the lungs of these individuals who have allergic asthma and that abrogate tolerance are not yet clear, but we suggest that tolerogenic pDC repertoire and/or function in these individuals might be altered. Acting on population of tolerogenic DCs such as CD8 α ⁺β⁻ and CD8 α ⁺β⁺ pDCs capable to induce antigen-specific regulatory T cell can restore immune tolerance to allergens. As a result, the identification of cells with tolerogenic functions is of great interest for the design of interventional approaches to control disorders related to an imbalance in immunological tolerance such as allergy and autoimmune diseases.

Only few reports described subpopulation of pDCs. For instance, CCR9 and CD9 expression were shown to define subsets of murine pDCs.^{13,36} However, CCR9⁻ and CD9⁺ pDCs do not display all the specific markers of terminally differentiated pDCs in contrast with the three subsets of pDCs described

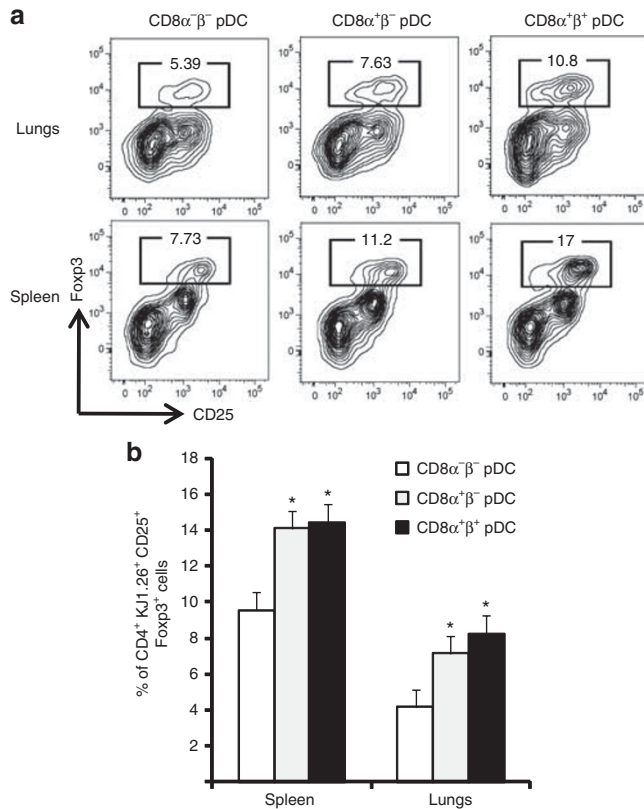


Figure 6 CD8 α ⁺β⁻ and CD8 α ⁺β⁺ plasmacytoid dendritic cells (pDCs) promote the conversion of naïve CD4⁺ T cells into CD4⁺ CD25⁺ Foxp3⁺ T cells *in vivo*. (a) pDC subsets were sorted from peripheral lymph nodes of Fms-like tyrosine kinase 3-ligand (Flt3-L)-treated mice, loaded with ovalbumin (OVA) (4 h in the presence of 10 μg ml⁻¹ OVA) and co-transferred by intravenous injection with naïve OVA-specific CD4⁺ T cells (3 × 10⁵ pDCs and 3 × 10⁶ CD4⁺ CD62L⁺ Foxp3⁻ T cells) into naïve BALB/c mice. After 4 days, mice were challenged by intranasal administration of OVA (50 μg in phosphate-buffered saline (PBS)). At day 5, spleen and lung were harvested and expression of Foxp3 was analyzed in individual mouse by flow cytometry in CD3⁺ CD4⁺ KJ1.26⁺ CD25⁺ cells. Results shown are representative dot plots and (b) mean ± s.e.m. of two independent experiments performed with groups of three mice. *P < 0.05 as calculated with Student's *t*-test.

Figure 5 CD8 α ⁺β⁻ and CD8 α ⁺β⁺ plasmacytoid dendritic cells (pDCs) prevent the development of airway hyper-reactivity (AHR). (a) CD8 α ⁻β⁻, CD8 α ⁺β⁻, and CD8 α ⁺β⁺ pDCs sorted by flow cytometry from peripheral lymph nodes of Fms-like tyrosine kinase 3-ligand (Flt3-L)-treated mice were loaded with ovalbumin (OVA) (10 μg ml⁻¹) for 4 h. Cells were then adoptively transferred into naïve BALB/c mice (2 × 10⁵ cells per mouse). At day 7, mice were immunized by intraperitoneal (IP) injection of OVA (50 μg) in aluminum hydroxide (Alum) (2 mg) and challenged at days 14, 15, and 16 by intranasal (IN) administration of OVA (50 μg in 50 μl saline). (b) At day 17, AHR was assessed by measurement of lung resistance and dynamic compliance by invasive plethysmography. Results are the mean ± s.e.m. of five mice groups of one representative experiment out of two. *P < 0.05 as calculated with Student's *t*-test. (c) Representative lung histology of mice from panel b. Lung tissue from mice transferred with CD8 α ⁻β⁻, CD8 α ⁺β⁻, and CD8 α ⁺β⁺ pDCs or saline were stained with hematoxylin and eosin (H&E, upper panel) and periodic acid Schiff (PAS, lower panel). Arrows show the release of the mucus in the lumen (original magnification ×200, inset ×600). (d) A suspension of lung cells was prepared after enzymatic digestion of lungs and isolation of leukocytes by density gradient centrifugation and positive selection using CD45 microbeads. Lung leukocytes were then plated and restimulated with OVA (100 μg ml⁻¹) for 3 days. Culture supernatants were harvested and tested for interleukin (IL)-4 and IL-13 by enzyme-linked immunosorbent assay (ELISA). (e) Sera were collected on day 17 and OVA-specific immunoglobulin (Ig)E and IgG levels were determined by ELISA. *P < 0.05 compared to OVA-sensitized mice (OVA). PBS, phosphate-buffered saline.

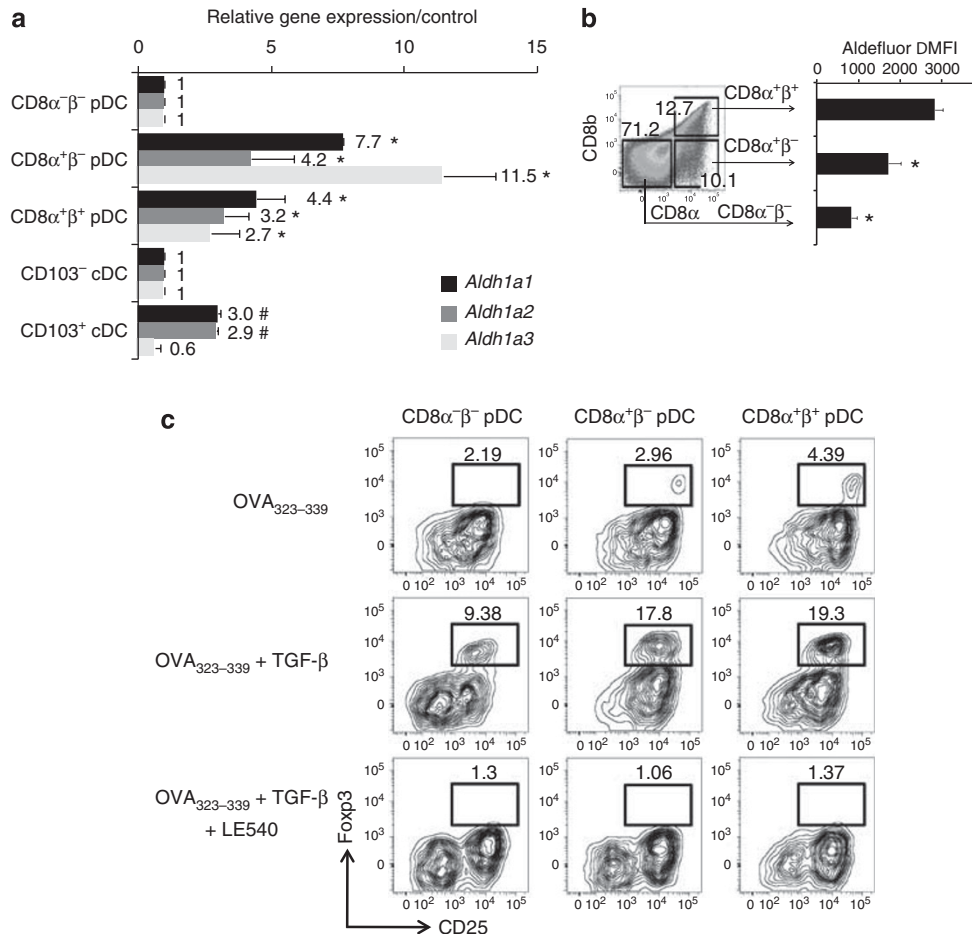


Figure 7 CD8 α ⁺β⁻ and CD8 α ⁺β⁺ plasmacytoid dendritic cells (pDCs) exhibit high retinal dehydrogenase (RALDH) activity and promote the differentiation of CD4⁺CD25⁺ Foxp3⁺ T cells *in vitro* in a transforming growth factor-β (TGF-β)- and retinoic acid-dependent manner. (a) Gene expression of *Aldh1a1*, *Aldh1a2*, and *Aldh1a3* was assessed by real-time PCR in CD8 α ⁻β⁻, CD8 α ⁺β⁻, and CD8 α ⁺β⁺ pDCs from peripheral lymph nodes or in CD103⁻ and CD103⁺ DCs from mesenteric lymph nodes of Fms-like tyrosine kinase 3-ligand (Flt3-L)-treated mice. Data are mean ± s.e.m. of two independent experiments. *P*-values were calculated with Student's *t*-test. **P*-value < 0.05 (CD8 α ⁺β⁻ pDC and CD8 α ⁺β⁺ pDC compared to CD8 α ⁻β⁻). #*P*-value < 0.05 (CD103⁺ cDC compared to CD103⁻ cDC). (b) pDCs were incubated for 45 min at 37 °C in the presence of Aldefluor substrate with or without diethylaminobenzaldehyde (DEAB, RALDH inhibitor) to determine background staining. Cells were subsequently stained with anti-CD11c, anti-mPDCA1, anti-CD8 α , and anti-CD8 β antibodies, and analyzed by flow cytometry to detect RALDH activity. Values are average of (MFI without RALDH inhibitor) – (MFI with RALDH inhibitor) ± s.e.m. of three separate experiments. (c) Naïve ovalbumin (OVA)₃₂₃₋₃₃₉-specific CD4⁺ T cells were cultured with CD8 α ⁻β⁻, CD8 α ⁺β⁻, or CD8 α ⁺β⁺ pDCs at a 1:10 ratio (pDC:T CD4⁺) for 5 days in the presence of OVA₃₂₃₋₃₃₉ peptide with or without TGF-β (1 ng ml⁻¹) or LE540 (1 μM) as indicated. Cells were subsequently stained with CD3, CD4, and CD25 antibodies, fixed, permeabilized, and stained for intracellular Foxp3 before flow cytometry analysis. Foxp3 expression was analyzed among CD3⁺CD4⁺CD25⁺ cells; dot plots are representative of three independent experiments. *P*-values were calculated with Student's *t*-test. **P*-value < 0.05 (CD8 α ⁺β⁻ and CD8 α ⁺β⁺ compared to CD8 α ⁻β⁻).

in this study. Interestingly, CCR9⁺ pDCs exhibit tolerogenic properties *in vitro* and *in vivo*,¹³ but we determined by flow cytometry that either the immunogenic (CD8 α ⁻β⁻) or the tolerogenic subsets (CD8 α ⁺β⁻ and CD8 α ⁺β⁺) of pDCs we have described express comparable levels of CCR9 (data not shown). Another difference is that CCR9⁺ pDCs downregulate CCR9 after activation with TLR ligands, whereas the pDC subsets we have defined according to CD8 α and CD8 β expression are not altered after TLR engagement. CD8 α was originally reported in mice to be expressed on a subset of cDCs characterized by their ability to produce high quantities of IL-12, to capture dead cells and to cross-present antigens.³⁷ Our data reveal that mouse pDCs can not only express CD8 α , but also

CD8 β . Both cDCs and pDCs expressing CD8 α share several properties such as strong antigen uptake ability, weak capacity to prime CD4⁺ T cells, and tolerogenic features.^{38,39} However, the functional human counterpart of mouse CD8 α ⁺ cDCs recently described to express CD141 (BDCA3) do not display a plasmacytoid phenotype.⁴⁰⁻⁴³ To translate our findings to human, further investigations are required to identify markers defining the human equivalent of mouse CD8 α ⁺β⁻ and CD8 α ⁺β⁺ pDCs.

Expression of *Aldh* genes was greatly increased in tolerogenic CD8 α ⁺β⁻ and CD8 α ⁺β⁺ pDC subsets and correlated with RALDH activity as determined with a fluorescent substrate, Aldefluor, by flow cytometry. It has previously been

demonstrated that RALDH activity in specific subsets of APCs is increased at mucosal sites.^{15,20,21,44,45} This is thought to be associated with the requirement for the induction of tolerance at these sites owing to the constant exposure to innocuous antigens. In mucosal APCs, expression of RALDH and the subsequent production of retinoic acid are vital for the induction of T-cell tolerance and induction of T_{reg} cells.^{15,31} Interestingly, tolerogenic cDCs from the gut express only two isoforms of RALDH (RALDH1 and 2),^{44–46} whereas the tolerogenic pDC subsets reported herein have increased expression of RALDH3 in addition to RALDH1 and 2. The expression of RALDH3 in tolerogenic subsets of APCs was not reported earlier, suggesting that all the enzymes involved in the biosynthesis of retinoic acid can be considered as a suitable marker of DCs with the ability to promote the generation of Foxp3⁺ CD4⁺ T cells. When we inhibited RALDH activity *in vitro*, the capacity of tolerogenic pDCs to induce conversion on naïve CD4⁺ T cells into Foxp3⁺ T_{reg} cells was greatly diminished. Therefore, targeting RALDH activity would allow for the manipulation of tolerance induction by pDCs in allergic diseases, autoimmunity, or in repression of immunological tolerance to cancer cells.

In conclusion, here we have used several molecular and cellular approaches, to segregate tolerogenic pDCs from other DCs. We have shown that the expression of CD8 α and in particular CD8 α and CD8 β designate new subsets of tolerogenic pDCs with the capacity to induce the differentiation of Foxp3⁺ T_{reg} cells and are very effective in suppressing AHR. The induction of T_{reg} cells was dependent on retinoic acid and TGF- β . Therefore, strategies to expand or activate tolerogenic pDC subsets might therefore have an important role in the induction and maintenance of peripheral tolerance. Thus, future studies to explore the possibility of targeting tolerogenic pDC subsets *in vivo* to use them for therapeutic purposes will benefit a wide range of inflammatory disorders, including autoimmunity, allergic disorders, and transplantation.

METHODS

Mice. Female BALB/c ByJ mice and B6(Cg)-Tg(B2m)1Trg Tg(HLA-B)1Trg/Dcr (B2m^{-/-}) mice (all 6–8 weeks old) were purchased from The Jackson Laboratory (Bar Harbor, ME). All mice were maintained in a pathogen-free mouse colony at the Keck School of Medicine (University of Southern California) under protocols approved by the Institutional Animal Care and Use Committee.

Flow cytometry. Cells were pre-incubated with normal rat serum and washed before staining. Subsets of DCs were identified using various antibody combinations, including anti-B220 APC-Cy7 (RA3-6B2), anti-CD40 FITC (3/23), anti-CD80 FITC (16-10A1), anti-CD86 PerCP-Cy5.5 (GL1), anti-IA/IE eFluor450 (M5/114.15.2), anti-Ly6c PerCP-Cy5.5 (HK1.4), anti-CD8 α PE-Cy7 (53-6.7), anti-CD8 β APC (H35-17.2 or 53-5.8), anti-CD3 PerCP-Cy5.5 (145-2C11), anti-PD-L1 FITC (MIH5; all from BD Biosciences, San Jose, CA), Siglec-H FITC (eBio440c), anti-ICOS-L PE (HK5.3), anti-CD11c eFluor450 (N418), anti-PD-L2 PE (122; all from eBioscience, San Diego, CA), anti-mPDCA1 FITC or PE (Miltenyi Biotec, Auburn, CA), and anti-Ly49Q PE (2E6; MBL International, Woburn, MA). The cells were washed with cold phosphate-buffered saline (PBS) + 2% fetal calf serum and acquired

with an 8-color FACS Canto II flow cytometer (BD Biosciences). The data were analyzed using the FlowJo 6.2 software (Tree Star, Ashland, OR).

pDC isolation and cell sorting. To prepare single-cell suspension, peripheral lymph nodes (cervical and inguinal lymph nodes pooled) were digested with 1.6 mg ml⁻¹ collagenase (CLS4; Worthington Biochemicals, Lakewood, NJ) and 0.1% DNase I (Fraction IX; Sigma, St Louis, MO) at 37°C on an orbital shaker for 15 min, and for an additional 15 min after passing it multiple times through an 18-gauge needle. For *in vivo* expansion of DCs, we prepared Renca (BALB/c renal carcinoma cell line) cells expressing Flt3-L^{23,47,48} and subcutaneously injected 5 \times 10⁶ cells into BALB/c mice. For B2m^{-/-} mice, we used B16 melanoma expressing Flt3-L as described previously.²³ After 14 days, peripheral lymph nodes were harvested and processed as described above. To isolate pDCs, cells were labeled with anti-mPDCA-1 microbeads (Miltenyi) and then positively sorted by AutoMACS according to the manufacturer's instruction. Purity of pDCs was always >95%. pDC subsets were identified based on CD11c and mPDCA1 staining; CD8 α ⁻ β ⁻, CD8 α ⁺ β ⁻, and CD8 α ⁺ β ⁺ pDC subsets were sorted using a FACS ARIA III cell sorter (BD Biosciences).

Confocal microscopy. pDCs were sorted as described above and cells were stained for surface markers with the following antibodies: anti-CD8 α Cy5 (53-6.7), anti-CD8 β TRITC (H35-17.2, both from eBioscience), and either anti-IA/IE (M5/114.15.2), anti-CD11c (HL3; all from BD Bioscience), or mPDCA1 (Miltenyi) antibodies conjugated to FITC. Cells were subsequently fixed and permeabilized using the BD Biosciences Fix/Perm solution. Washed cells were mounted onto slides in Vectashield mounting medium (Vector Laboratories, Burlingame, CA). Images were acquired with a Nikon Eclipse Ti confocal microscope (Nikon, Instruments, Melville, NY) using a \times 100 oil objective associated to the Nikon EC-Z1 software.

Quantitative real-time PCR. Total RNA was extracted from sorted subtypes of pDCs using the RNAasy mini kit (Qiagen, Valencia, CA) and cDNAs were generated with the High Capacity cDNA Reverse Transcription Kit (Applied Biosystems, Carlsbad, CA) according to the manufacturer's recommendations. Quantification of mRNA levels was carried out by quantitative real-time PCR on a CFX96 thermal cycler (Bio-Rad, Hercules, CA) with predesigned Taqman gene expression assays for *Actb* (Mm0060732_m1), *Cd8a* (Mm01182108_m1), *Cd8b* (Mm00438116_m1), *Aldh1a1* (Mm00657317_m1), *Aldh1a2* (Mm00657317_m1), and *Aldh1a3* (Mm00474049_m1) (Applied Biosystems,) and reagents, as per the manufacturer's instructions. Results were analyzed using the comparative C(T) method (2^{- $\Delta\Delta$ C(T)} method).⁴⁹

Sensitization and tolerance models and measurement of airway responsiveness. CD8 α ⁻ β ⁻, CD8 α ⁺ β ⁻, and CD8 α ⁺ β ⁺ purified pDCs were isolated from pooled peripheral lymph nodes of BALB/mice treated with Flt3-L-producing cells. Each subset was loaded with OVA (10 μ g ml⁻¹) for 4 h at 37°C. Cells were subsequently washed two times and resuspended in saline solution. For the sensitization model, 2 \times 10⁵ cells (pDCs or bone marrow-derived DCs prepared as described previously⁵⁰) were adoptively transferred by intravenous injection through the tail vein. At 7 days after the transfer, mice were challenged on three consecutive days by intranasal administration of OVA (50 μ g in PBS). For the tolerance model, OVA-loaded pDC subsets were adoptively transferred 7 days prior intraperitoneal injection of OVA (50 μ g) in aluminum hydroxide (Alum, 2 mg), and subsequently recipients were challenged intranasally with three consecutive doses of OVA (50 μ g in PBS) on days 14, 15, and 16. AHR responses were subsequently assessed by methacholine-induced airflow obstruction in conscious mice placed in a whole-body plethysmograph (Buxco Electronics, Troy, NY) as described before⁵¹ or by invasive measurement of airway resistance, in which anesthetized and

tracheostomized mice were ventilated mechanically.⁵² Briefly, aerosolized methacholine was administered in increasing concentrations of methacholine (0, 1.25, 2.5, 5, and 10 mg ml⁻¹) and we continuously computed the lungs' resistance and dynamic compliance by fitting flow, volume, and pressure to an equation of motion. AHR was measured at 24 h after the last intranasal challenge. Alternatively, sera were isolated to test OVA-specific immunoglobulin E and immunoglobulin G levels by enzyme-linked immunosorbent assay (ELISA) (MD Bioproducts, St Paul, MN and My Biosource, San Diego, CA, respectively).

Lung histology. Transcardial perfusion of lungs was performed with cold PBS and subsequently lungs were harvested for histology and fixed with 4% paraformaldehyde buffered in PBS. After fixation, the lungs were embedded in paraffin, cut into 4 μm sections, and stained with hematoxylin and eosin and periodic acid Schiff according to standard procedures. Histology pictures were acquired using a DFC290 Leica camera (Leica Microsystems, Bannockburn, IL).

Analysis of RALDH activity by flow cytometry. The activity of RALDH enzymes was determined using the Aldefluor staining kit (StemCell Technologies, Vancouver, BC, Canada). pDCs were isolated from pooled peripheral lymph nodes and incubated for 45 min at 37°C in the presence of different dilution of BODIPY-aminoacetaldehyde diethyl acetal (Aldefluor substrate) with or without RALDH inhibitor DEAB. Cells were subsequently stained for mPDCA1, CD11c, CD8α, and CD8β and analyzed by flow cytometry.

In vitro culture. Sorted subpopulation of pDCs were cultured for 24 h in the presence of CpG 1826 (1 μM; Invivogen, San Diego, CA), R848 (1 μg ml⁻¹; Alexis Biochemicals, San Diego, CA), or medium only. Supernatants were then harvested for further measurement of cytokine production by ELISA for IFN-α (PBL Interferon Source, Piscataway, NJ), IL-6, tumor necrosis factor-α, and IL-10 (eBioscience). Alternatively, to test the antigen uptake capacity of pDC subsets, pDCs were incubated with OVA-APC (Invitrogen, Carlsbad, CA) for 60, 120, or 180 min at 4°C or 37°C and then analyzed by flow cytometry. To test the ability of pDC subpopulations to prime naïve CD4⁺ T cells, CD8α⁻β⁻ pDCs, CD8α⁺β⁻ pDCs, and CD8α⁺β⁺ pDCs were co-cultured with naïve CD4⁺ T cells from DO11.10 mice in the presence of OVA (10 μg ml⁻¹) for 3 days at a 1:10 ratio (1 × 10⁴ pDCs/1 × 10⁵ T cells) in a 96-well round bottom plate. Naïve CD4⁺ T cells were purified from spleen of DO11.10 mice using the CD4⁺ CD62L⁺ T Cell Isolation Kit II (Miltenyi) following the manufacturer's recommendations. The purity of sorted naïve CD4⁺ T cells was consistently above 95%. Cells were then pulsed with tritiated thymidine (1 μCi per well) for 18 h and proliferation was evaluated using a beta-counter (Beckman Coulter, Brea, CA) as described earlier.¹ Alternatively, supernatants were harvested to measure IL-2 production by ELISA (eBioscience). To evaluate the production of Th2 cytokines in lungs of OVA-Alum-sensitized mice treated with the different pDC subsets, a single-cell suspension was prepared from lungs as described previously.⁵³ From this cell suspension, leukocytes were positively sorted using CD45 microbeads (Miltenyi). CD45⁺ cells were then plated in a 96-well plate round bottom (2 × 10⁵ cells per well) and restimulated for 3 days with OVA (100 μg ml⁻¹). Supernatants were harvested and tested for IL-4 and IL-13 by ELISA (eBioscience). To assess induction of Foxp3 in naïve CD4⁺ T cells, pDC subsets were co-cultured with naïve CD4⁺ CD62L⁺ Foxp3⁻ T cells isolated from DO11.10 mice at a 1:10 ratio (1 × 10⁴ pDCs/1 × 10⁵ T cells) in a 96-well round bottom plate. Medium was supplemented with OVA peptide (OVA₃₂₃₋₃₃₉, 1 μg ml⁻¹; Peptides International, Louisville, KY), anti-IL-12 (C17.8), anti-IL-4 (11.B11), anti-IFN-γ (XMG1.2), and anti-IL-6 (MP5-20F3) antibodies (all at 10 μg ml⁻¹; Bioxcell, West Lebanon, NH), with TGF-β (1 ng ml⁻¹; eBioscience) and/or LE540 (1 μM; Wako Chemicals, Richmond, VA). After 5 days of culture, cells were harvested, washed, and stained to assess Foxp3 expression using the FJK-16s Foxp3-specific clone (eBioscience) and the Foxp3 Staining Buffet Set (eBioscience) according to the manufacturer's instructions.

Induction of antigen-specific Foxp3⁺ T cells by pDC subsets *in vivo*.

To test the ability of pDC subsets to generate Foxp3⁺ T cells *in vivo*, OVA-loaded CD8α⁻β⁻, CD8α⁺β⁻, or CD8α⁺β⁺ purified pDCs were adoptively transferred along with naïve OVA-specific CD4⁺ T cells as mentioned above (3 × 10⁵ pDCs and 3 × 10⁶ CD4⁺ CD62L⁺ Foxp3⁻ T cells) into naïve BALB/c mice. Mice were challenged at day 4 by intranasal administration of OVA (50 μg in PBS) and killed the following day. Expression of Foxp3 was evaluated by flow cytometry in CD3⁺ CD4⁺ KJ1.26⁺ CD25⁺ T cells from spleen and lungs.

Statistical analysis. Differences between groups were analyzed by two-tailed, unpaired, Student's *t*-test and considered significant when the *P*-value was <0.05.

SUPPLEMENTARY MATERIAL is linked to the online version of the paper at <http://www.nature.com/mi>

ACKNOWLEDGMENTS

This work was supported by the NIH R01 AI066020 grant. V.L. is supported by a Senior Research Training Fellowship from the American Lung Association.

DISCLOSURE

The authors declared no conflict of interest.

© 2012 Society for Mucosal Immunology

REFERENCES

- Akbari, O., DeKruyff, R.H. & Umetsu, D.T. Pulmonary dendritic cells producing IL-10 mediate tolerance induced by respiratory exposure to antigen. *Nat. Immunol.* **2**, 725–731 (2001).
- Coquerelle, C. & Moser, M. DC subsets in positive and negative regulation of immunity. *Immunity. Rev.* **234**, 317–334 (2010).
- Medzhitov, R. & Janeway, C.A. Jr Decoding the patterns of self and nonself by the innate immune system. *Science* **296**, 298–300 (2002).
- Palucka, K., Banchereau, J. & Melman, I. Designing vaccines based on biology of human dendritic cell subsets. *Immunity* **33**, 464–478 (2010).
- Pulendran, B., Tang, H. & Manicassamy, S. Programming dendritic cells to induce T(H)2 and tolerogenic responses. *Nat. Immunol.* **11**, 647–655 (2010).
- Steinman, R.M., Hawiger, D. & Nussenzweig, M.C. Tolerogenic dendritic cells. *Annu. Rev. Immunol.* **21**, 685–711 (2003).
- Shortman, K. & Liu, Y.J. Mouse and human dendritic cell subtypes. *Nat. Rev. Immunol.* **2**, 151–161 (2002).
- Colonna, M., Trinchieri, G. & Liu, Y.J. Plasmacytoid dendritic cells in immunity. *Nat. Immunol.* **5**, 1219–1226 (2004).
- Gilliet, M., Cao, W. & Liu, Y.J. Plasmacytoid dendritic cells: sensing nucleic acids in viral infection and autoimmune diseases. *Nat. Rev. Immunol.* **8**, 594–606 (2008).
- de Heer, H.J. *et al.* Essential role of lung plasmacytoid dendritic cells in preventing asthmatic reactions to harmless inhaled antigen. *J. Exp. Med.* **200**, 89–98 (2004).
- Kool, M. *et al.* An anti-inflammatory role for plasmacytoid dendritic cells in allergic airway inflammation. *J. Immunol.* **183**, 1074–1082 (2009).
- Goubier, A. *et al.* Plasmacytoid dendritic cells mediate oral tolerance. *Immunity* **29**, 464–475 (2008).
- Hadeiba, H. *et al.* CCR9 expression defines tolerogenic plasmacytoid dendritic cells able to suppress acute graft-versus-host disease. *Nat. Immunol.* **9**, 1253–1260 (2008).
- Ochando, J.C. *et al.* Alloantigen-presenting plasmacytoid dendritic cells mediate tolerance to vascularized grafts. *Nat. Immunol.* **7**, 652–662 (2006).
- Coombes, J.L. *et al.* A functionally specialized population of mucosal CD103⁺ DCs induces Foxp3⁺ regulatory T cells via a TGF-β and retinoic acid-dependent mechanism. *J. Exp. Med.* **204**, 1757–1764 (2007).
- Akbari, O. *et al.* Antigen-specific regulatory T cells develop via the ICOS-ICOS-ligand pathway and inhibit allergen-induced airway hyperreactivity. *Nat. Med.* **8**, 1024–1032 (2002).

17. Lloyd, C.M. & Murdoch, J.R. Tolerizing allergic responses in the lung. *Mucosal Immunol.* **3**, 334–344 (2010).
18. Stock, P. *et al.* Induction of T helper type 1-like regulatory cells that express Foxp3 and protect against airway hyper-reactivity. *Nat. Immunol.* **5**, 1149–1156 (2004).
19. Sun, C.M. *et al.* Small intestine lamina propria dendritic cells promote *de novo* generation of Foxp3 T reg cells via retinoic acid. *J. Exp. Med.* **204**, 1775–1785 (2007).
20. Manicassamy, S. & Pulendran, B. Retinoic acid-dependent regulation of immune responses by dendritic cells and macrophages. *Semin. Immunol.* **21**, 22–27 (2009).
21. Williams, M. *et al.* Skin-draining lymph nodes contain dermis-derived CD103(–) dendritic cells that constitutively produce retinoic acid and induce Foxp3(+) regulatory T cells. *Blood* **115**, 1958–1968 (2010).
22. Hammad, H. *et al.* Inflammatory dendritic cells—not basophils—are necessary and sufficient for induction of Th2 immunity to inhaled house dust mite allergen. *J. Exp. Med.* **207**, 2097–2111 (2010).
23. Mach, N. *et al.* Differences in dendritic cells stimulated *in vivo* by tumors engineered to secrete granulocyte–macrophage colony-stimulating factor or Flt3-ligand. *Cancer Res.* **60**, 3239–3246 (2000).
24. Vremec, D., Pooley, J., Hochrein, H., Wu, L. & Shortman, K. CD4 and CD8 expression by dendritic cell subtypes in mouse thymus and spleen. *J. Immunol.* **164**, 2978–2986 (2000).
25. Koller, B.H., Marrack, P., Kappler, J.W. & Smithies, O. Normal development of mice deficient in beta 2M, MHC class I proteins, and CD8+ T cells. 1990. *J. Immunol.* **184**, 4592–4595 (2010).
26. Hochrein, H., O’Keeffe, M. & Wagner, H. Human and mouse plasmacytoid dendritic cells. *Hum. Immunol.* **63**, 1103–1110 (2002).
27. Konieczna, P. *et al.* Bifidobacterium infantis 35,624 administration induces Foxp3 T regulatory cells in human peripheral blood: potential role for myeloid and plasmacytoid dendritic cells. *Gut* **61**, 354–366 (2012).
28. Tokita, D. *et al.* Poor allostimulatory function of liver plasmacytoid DC is associated with pro-apoptotic activity, dependent on regulatory T cells. *J. Hepatol.* **49**, 1008–1018 (2008).
29. Sakaguchi, S., Wing, K., Onishi, Y., Prieto-Martin, P. & Yamaguchi, T. Regulatory T cells: how do they suppress immune responses? *Int. Immunol.* **21**, 1105–1111 (2009).
30. Haskins, K. *et al.* The major histocompatibility complex-restricted antigen receptor on T cells. I. Isolation with a monoclonal antibody. *J. Exp. Med.* **157**, 1149–1169 (1983).
31. Mucida, D. *et al.* Reciprocal TH17 and regulatory T cell differentiation mediated by retinoic acid. *Science* **317**, 256–260 (2007).
32. Stock, A., Booth, S. & Cerundolo, V. Prostaglandin E2 suppresses the differentiation of retinoic acid-producing dendritic cells in mice and humans. *J. Exp. Med.* **208**, 761–773 (2011).
33. Li, Y., Hashimoto, Y., Agadir, A., Kagechika, H. & Zhang, X. Identification of a novel class of retinoic acid receptor beta-selective retinoid antagonists and their inhibitory effects on AP-1 activity and retinoic acid-induced apoptosis in human breast cancer cells. *J. Biol. Chem.* **274**, 15360–15366 (1999).
34. Izcue, A., Coombes, J.L. & Powrie, F. Regulatory T cells suppress systemic and mucosal immune activation to control intestinal inflammation. *Immunol. Rev.* **212**, 256–271 (2006).
35. Lambrecht, B.N. & Hammad, H. The role of dendritic and epithelial cells as master regulators of allergic airway inflammation. *Lancet* **376**, 835–843 (2010).
36. Bjorck, P., Leong, H.X. & Engleman, E.G. Plasmacytoid dendritic cell dichotomy: identification of IFN-alpha producing cells as a phenotypically and functionally distinct subset. *J. Immunol.* **186**, 1477–1485 (2011).
37. Villadangos, J.A. & Shortman, K. Found in translation: the human equivalent of mouse CD8+ dendritic cells. *J. Exp. Med.* **207**, 1131–1134 (2010).
38. Shortman, K. & Heath, W.R. The CD8+ dendritic cell subset. *Immunol. Rev.* **234**, 18–31 (2010).
39. Wang, L. *et al.* Programmed death 1 ligand signaling regulates the generation of adaptive Foxp3+CD4+ regulatory T cells. *Proc. Natl. Acad. Sci. USA* **105**, 9331–9336 (2008).
40. Bachem, A. *et al.* Superior antigen cross-presentation and XCR1 expression define human CD11c+CD141+ cells as homologues of mouse CD8+ dendritic cells. *J. Exp. Med.* **207**, 1273–1281 (2010).
41. Contreras, V. *et al.* Existence of CD8alpha-like dendritic cells with a conserved functional specialization and a common molecular signature in distant mammalian species. *J. Immunol.* **185**, 3313–3325 (2010).
42. Jongbloed, S.L. *et al.* Human CD141+ (BDCA-3)+ dendritic cells (DCs) represent a unique myeloid DC subset that cross-presents necrotic cell antigens. *J. Exp. Med.* **207**, 1247–1260 (2010).
43. Poulin, L.F. *et al.* Characterization of human DNGR-1+ BDCA3+ leukocytes as putative equivalents of mouse CD8alpha+ dendritic cells. *J. Exp. Med.* **207**, 1261–1271 (2010).
44. Denning, T.L., Wang, Y.C., Patel, S.R., Williams, I.R. & Pulendran, B. Lamina propria macrophages and dendritic cells differentially induce regulatory and interleukin 17-producing T cell responses. *Nat. Immunol.* **8**, 1086–1094 (2007).
45. Manicassamy, S. *et al.* Activation of beta-catenin in dendritic cells regulates immunity vs. tolerance in the intestine. *Science* **329**, 849–853 (2010).
46. Molenaar, R. *et al.* Expression of retinaldehyde dehydrogenase enzymes in mucosal dendritic cells and gut-draining lymph node stromal cells is controlled by dietary vitamin A. *J. Immunol.* **186**, 1934–1942 (2011).
47. Lyman, S.D. *et al.* Molecular cloning of a ligand for the flt3/flk-2 tyrosine kinase receptor: a proliferative factor for primitive hematopoietic cells. *Cell* **75**, 1157–1167 (1993).
48. Murphy, G.P. & Hrushesky, W.J. A murine renal cell carcinoma. *J. Natl. Cancer Inst.* **50**, 1013–1025 (1973).
49. Schmittgen, T.D. & Livak, K.J. Analyzing real-time PCR data by the comparative C(T) method. *Nat. Protoc.* **3**, 1101–1108 (2008).
50. Inaba, K. *et al.* Generation of large numbers of dendritic cells from mouse bone marrow cultures supplemented with granulocyte/macrophage colony-stimulating factor. *J. Exp. Med.* **176**, 1693–1702 (1992).
51. Akbari, O. *et al.* Essential role of NKT cells producing IL-4 and IL-13 in the development of allergen-induced airway hyperreactivity. *Nat. Med.* **9**, 582–588 (2003).
52. Akbari, O. *et al.* ICOS/ICOSL interaction is required for CD4+ invariant NKT cell function and homeostatic survival. *J. Immunol.* **180**, 5448–5456 (2008).
53. Stock, P., Lombardi, V., Kohlrantz, V. & Akbari, O. Induction of airway hyperreactivity by IL-25 is dependent on a subset of invariant NKT cells expressing IL-17RB. *J. Immunol.* **182**, 5116–5122 (2009).